Polynomial fitting functions for visible light positioning based on RSS with tilted receiver

Cristobal Carreño, Fabián Seguel, Patrick Charpentier, Nicolas Krommenacker

Polynomial Fitting Functions for Visible Light Positioning based on RSS with Tilted Receiver

Cristóbal Carreño[1], Fabian Seguel[2], Patrick Charpentier[1] and Nicolas Krommenacker[1]

[1]*Lorraine University, CRAN,CNRS UMR 7039, Nancy, France*
[2]*Universidad de Santiago de Chile, Department of Electrical Engineering, Santiago, Chile*

Abstract

In this work, we present the construction and comparison of three multivariate fitting functions to model the relation between received signal strength (RSS) and tilted receiver angle for 2-D visible light positioning systems. The performance of the different functions has been analysed by simulations for a mobile node. The tilted angle has been obtained from an inertial measurement unit (IMU) sensor considering his deviation from experimental measurements. This mismatch measurement is introduced in the Monte-Carlo simulation to measure its impact on the position estimation. According to the results, third order polynomial function overcomes first and second-order polynomial functions achieving a 0.16 m accuracy error.

Keywords

Visible Light Positioning, Tilted Photodiode, Polynomial Fitting, Inertial Measurement Unit, Received Signal Strength.

1. Introduction

Positioning information has become an important issue every day. An example of this is the Global Positioning System (GPS), and it is used for positioning and navigation services. GPS achieves great performance in outdoor environments. Nonetheless, this technology faces several issues when facing indoor environments. Satellites signals cannot penetrate the building's walls, producing distortion or shot down at communication link [1]. For solving this drawback, several indoor positioning systems (IPS) had been developed in the last decade. To provide IPS different technologies have been used Radiofrequency (RF), Ultrasound (US), and Visible light. RF is widely used but it is affected by the multi-path effect indoor and his signal produces interference with other RF signals, especially in areas as hospitals, airplanes or RF crowded. The US is affected to multi-path, depend strongly on room temperature and the Doppler shift effect causes several problems in the communication link. In recent years, the development of Visible Light Communications (VLC) has encouraged the research on positioning systems based on Optical Wireless Communications (OWC) technology. It has some advantages as No interference in RF crowded areas, deployed lamps at buildings can be used as transmitters, low energy consumption, and security aspects in indoor environments. These reasons have become

IPIN 2021 WiP Proceedings, November 29 – December 2, 2021, Lloret de Mar, Spain
carrenom1@univ-lorraine.fr (C. Carreño); fabian.seguelg@usach.cl (F. Seguel); patrick.charpentier@univ-lorraine.fr (P. Charpentier); nicolas.krommenacker@univ-lorraine.fr (N. Krommenacker)

VLC an attractive technology for IPS systems. [2].

The IPS based on VLC referred to as Visible Light Positioning systems (VLP) can be classified into two types according to the sensor used to capture visible light, namely, Image Sensor (IS) or Photodiode (PD). There is another sensor, photoresistor (PR) can be used on IPS, an example is in[3] but VLP advances have preferred PD over PR due to high data rates for communication proposes. Concerning IS sensors, they provide information from transmitters positioning to visions analysis algorithm, but they have big limitations in data rate. On the other hand, PDs provide information about optical power from lights and they have an easy hardware implementation but they need a transimpedance amplifier (TIA), in contrast with PRs is not needed. An example of going to work at a higher data rate of PD than IS is depicted in[4]. Another aspect of PD's is orientation changes produce an error on positioning estimation for VLP algorithms based on RSS because the trilateration technique depends on distance estimation between transmitters and receiver. The distance can be estimated using regression functions as shown in [5] that includes non-line-on-sight (NLOS) components, but without considering the PD inclination effect. Another example is presented in [6] but under the perspective of unknown transmitter orientation. Although the problem is the same, the angles transmitter are fixed in contrast with the orientation of PD which is variable. Another case is presented in [7] and his work is based on channel DC gain. Results demonstrate there exist changes at distance estimation due to the mobile user's dynamics. In [8] there is a mathematical analysis of influence receiver's orientation at a change of planar projection distances between transmitter and receiver. The error in the estimated distance is corrected introducing a planar distances bias from height and PD´s parameters. In [9, 10] is proposed a function to correct the received power and then correct the estimated distance. These functions correspond to a correction factor that depends on incident angle changes and is modeled by exponential functions that include PD's parameters. The problem with these functions is depending on the position of PD, and this is normally unknown. An alternative way is to approximate the incidence angle factor in the channel model and this is shown in [11], technique used there consists in constructs the incidence angle factor through functions of first and second order, but they are focused on incident angle and not of tilted angle. Another approach to overcome this drawback is to solve an optimization problem that identifies the position of PD observing changes between the ideal channel gain and the actual channel gain. The results are good but they still consider the tilted angle is always fixed. A different point of view is present in literature by using a multi-PD. In [12] four PDs are used to estimate the normal vector where the PDs are mounted. Normal vector has been modeled by multivariate Gaussian distribution, but the problem is there exists more information to process than in the case of one PD. Machine learning technique is used too with multi-PD in [13], where an artificial neural network (ANN) and Weighted K-Nearest Neighbour (WKNN) are programmed to recognize the patterns of RSS in each PD. The receiver's orientation is obtained through an inertial measurement unit (IMU). Then it seems the orientation problems are solved, but the IMU sensor is very susceptible to external forces, and magnetic fields for getting the angles, heuristic methods, complementary filtering, and Extended Kalman filter are few techniques used to overcome those problems [14, 15].

The approach of our work besides the fact it considers an inclined receiver with tilt angle

obtained from a real inertial sensor(IMU) including its uncertainty in the measure. The behavior of IMU has been characterized by variance and mean value of angle error. These values are used to build a Gaussian distribution function and incorporated on Monte-Carlo simulation [16, 17], with the proposal to train the polynomial functions for distance estimation and showing the performance of the entire positioning system. The paper is organized as follows: Section II will present the system model, the positioning system that includes, the fitting function definition, the optimization problem, and the trilateration equations. Section III is dedicated to present the parameters, IMU measurements distribution, and simulation results. Conclusions are presented in section IV.

2. System Model

The system is composed of four Transmitters (Lamps) and one mobile receiver in a square room with dimensions. Each lamps is separated from others to distance $D_x = D_y$ and height is h. The room is depicted in figure 1.

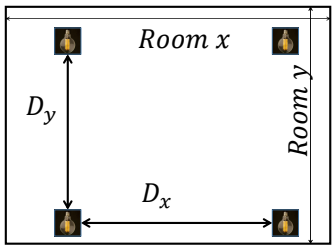

Figure 1: Room scenario

2.1. Channel Model

VLC channel is modelled considering the line of sight (LOS) components from each LED j in some mobile node´s point i. For simulation proposes make it easier, we consider the received power of PD only depends from the power of lamps and the noise present in receiver device (leaving out frequency responses of PD and LEDs, PD construction materials, ambient light effect, blockages scenarios or LED installation errors). The noise N is additive Gaussian $\mathcal{N}(0, \sigma^2)$ including shot and thermal noises. Noise expressions are available in [18]. Total power received corresponds to sum of power from every LED, this is showed in (1). R_p is the responsivity of PD, H_{ij}^{LOS} is the DC gain of LOS channel and P_j is the power transmitted for LED j. In (2) H_{ij}^{LOS} is obtained from the incidence angle ψ_{ij} and transmitter angle φ_{ij}, distance between transmitter and receiver d_{ij} and constant C_{ij}. DC gain is valid just when the incidence angles is less than PD's field of view (FOV) angle Ψ_l. C_{ij} depends of Lambertian order transmission m_l, the area of PD A and factors $G(\psi_{ij})$ and $T_s(\psi_{ij})$ that represents the optical filter gain and the optical concentrator in (3).

$$\sum_{j=1}^{4} P_{ij} = \sum_{j=1}^{4} R_p P_j H_{ij}^{LOS} + N \tag{1}$$

$$H_{ij}^{LOS} = \begin{cases} \frac{C_{ij}}{d_{ij}^2} \cos^{m_l}(\varphi_{ij}) \cos(\psi_{ij}) & 0 \leq \psi_{ij} \leq \Psi_l \\ 0 & \text{elsewhere} \end{cases} \tag{2}$$

$$C_{ij} = \frac{(m_l + 1)A}{2\pi} G(\psi_{ij}) T_s(\psi_{ij}) \tag{3}$$

The factor $\cos(\psi_{ji})$ is the same that $\cos(\varphi_{ij})$ when the normal vector of PD is perpendicular to ground plane. This is not the general case. We consider in this work a tilted PD, in consequence, it is necessary to find the $\cos(\psi_{ji})$ from tilted angle. This is possible from the expression in (4).Let be define $\cos(\psi_{ji})$ as the dot product between distance vector $\vec{d}_{ji}$ and tilted PD normal $\hat{N}_i$, divided by product of their norms. In spherical coordinates, the PD normal vector can be calculated from (5), where β is the tilt angle and α is the rotation angle. This work consider $\alpha = 0°$. The tilt angle β is delivered by an inertial sensor, because the PD can not knows this angle by itself. Figure 2 are showed the mentioned angles.

$$\cos(\psi_{ji}) = \frac{\vec{d}_{ji} \cdot \hat{N}_i}{\|\vec{d}_{ji}\|_2 \|\hat{N}_i\|_2} \tag{4}$$

$$\hat{N}_i = \frac{[\sin(\beta)\cos(\alpha), \sin(\beta)\sin(\alpha), \cos(\beta)]}{\|[\sin(\beta)\cos(\alpha), \sin(\beta)\sin(\alpha), \cos(\beta)]\|_2} \tag{5}$$

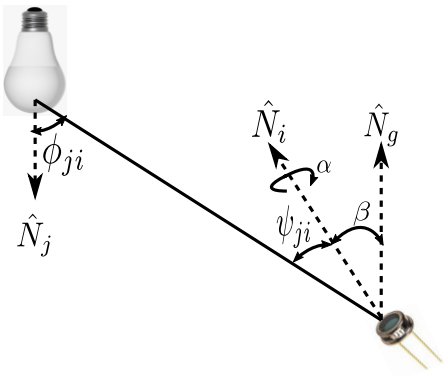

Figure 2: Tilted Photodiode

2.2. Positioning System

The transmitter send power square waves (without zero values) to the receiver with frequencies f_{mj}. This waves are modulated by sine functions with carrier frequencies f_{cj}. The displacement in frequency domain serves to mitigate the inter channel interference (ISI) and allowing to

separate the received signal in PD´s side from each LED. Once RSS is added with PD noise, Receiver apply four bandpass filter centred at frequencies f_{cj} and bandwidth $BW = 2f_{mj}$. A fast Fourier transform is used to obtain the RSS from each transmitter, using the Parseval's power theorem. With the transmitter identification by frequency of separated signal, the position of transmitter Tx_j is obtained. After that, IMU sensor delivers the tilted angle of PD. A fit function $f_j(\hat{v})$ of five variables (four powers and one angle) represented by vector $\vec{v}$ are used to estimate the distances to the LEDs from the PD $\hat{d}_j$, as showed in figure 3. Each $\hat{d}_j$ is employed to calculate the ratios $r_j = \sqrt{\hat{d}_j^2 - h^2}$. The matrices A in (6) and B in (7) correspond to trilateration technique and $x_j, j = 1, ..., 4$ $y_j, j = 1, ..., 4$ are the LEDs coordinates. Solution is obtained through Least Square Algorithm in (8).

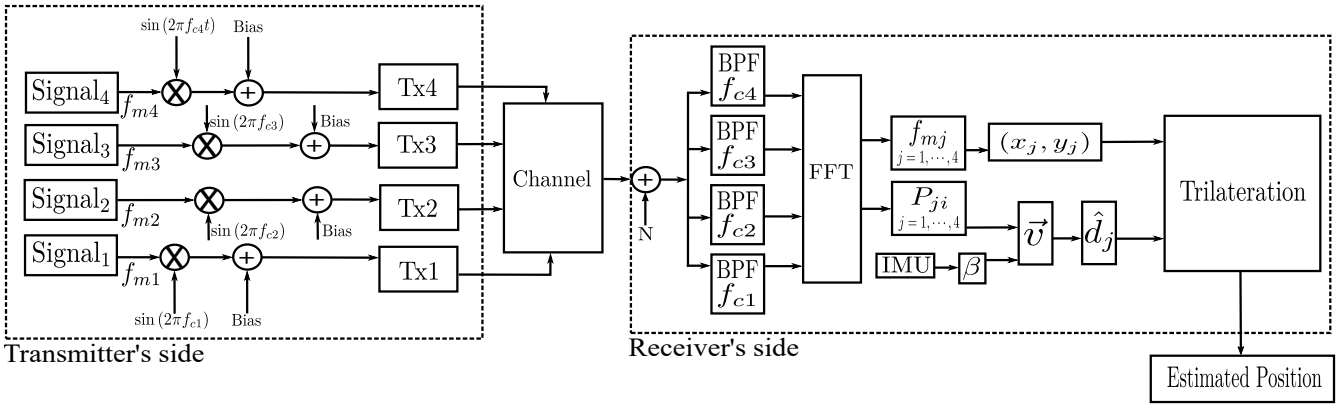

Figure 3: Positioning system description

$$A = \begin{bmatrix} x_2 - x_1 & y_2 - y_1 \\ x_3 - x_1 & y_3 - y_1 \\ x_4 - x_1 & y_4 - y_1 \end{bmatrix} \tag{6}$$

$$B = \begin{bmatrix} \left(r_1^2 - r_2^2\right) + \left(x_2^2 + y_2^2\right) - \left(x_1^2 + y_1^2\right) \\ \left(r_2^2 - r_3^2\right) + \left(x_3^2 + y_3^2\right) - \left(x_1^2 + y_1^2\right) \\ \left(r_1^2 - r_4^2\right) + \left(x_4^2 + y_4^2\right) - \left(x_1^2 + y_1^2\right) \end{bmatrix} \tag{7}$$

$$\hat{\vec{x}} = \left(A^\top A\right)^{-1} A^\top B \tag{8}$$

2.3. Distance Estimation

Distances calculation depend of the tilted angle of PD, which is delivered from IMU sensor and RSS. We define the vector $\vec{v} = (v_1, v_2, v_3, v_4, v_5) = (\hat{P}_{r1}, \hat{P}_{r2}, \hat{P}_{r3}, \hat{P}_{r4}, \beta_{imu})$ that contains all the information necessary for next step. To use all this data, we propose multidimensional polynomial functions $\hat{d}_j$ with argument vector $\vec{v}$. This functions can be constructed, with fist order terms, second order terms and third order terms. Second and third order terms come from the product combination among two or three variables. In (9) shows the third order polynomial function and that contains all other low order terms. Every term is multiplied by constants.

There are first order constants a_i , second order constants b_{ij} and third order constants c_{ijk} .Respect the terms $\sum a_i v_i$ corresponds to first order terms, $\sum b_{ij} v_j$ are the second order terms and $\sum v_i \sum v_j \sum c_{ijk} v_k$ are the third order terms. First and second order function are construct by deleting the second and third order terms respectively.

$$\hat{d}_j(\vec{v}) = a_0 + \sum_{i=1}^{5} a_i v_i + \sum_{i=1}^{5} v_i \sum_{j=1}^{i} b_{ij} v_j + \sum_{i=1}^{5} v_i \sum_{j=1}^{i} v_j \sum_{k=1}^{j} c_{ijk} v_k \tag{9}$$

It is necessary to find the constants in (9) to obtain the fitting functions, this step is called "Training Phase". To do this, we reorganise the terms in matrix form (10). Vector $\vec{g}$ in (11) represents all polynomial coefficients and they are the targets. Matrix D in (13) regroup all the terms. This matrix changes depends on the considered function. Each element in matrix D represents the data obtain from vector $\vec{v}$, if we consider n vectors $\vec{v}^{(n)}$, the Notation ${v_1}^{(n)}$ represents nth fist order terms, $v_1 \cdot {v_1}^{(n)} \dots v_5 \cdot {v_5}^{(n)}$ are the second order terms and $v_1 \cdot v_1 \cdot {v_1}^{(n)} \dots v_5 \cdot v_5 \cdot {v_5}^{(n)}$ the third order terms in D. F contains the values of d_j and they represent the perfect distance from PD to Tx_j. With vectors $\vec{g}$, F and matrix D, it is possible to solve the optimisation problem in (14) by Non linear least Square (NLLS) algorithm.

$$D \cdot (C)^T = F \tag{10}$$

$$\vec{g} = \begin{bmatrix} a_0 & a_1 & \cdots & a_5 & b_{11} & \cdots & b_{55} & c_{111} & \cdots & c_{555} \end{bmatrix} \tag{11}$$

$$F = \begin{bmatrix} d_j(\vec{v})^{(1)} & d_j(\vec{v})^{(2)} & \cdots & d_j(\vec{v})^{(n)} \end{bmatrix}^T \tag{12}$$

$$D = \begin{bmatrix} 1 & {v_1}^{(1)} & \cdots & {v_5}^{(1)} & v_1 \cdot {v_1}^{(1)} & \cdots & v_5 \cdot {v_5}^{(1)} & v_1 \cdot v_1 \cdot {v_1}^{(1)} & \cdots & v_5 \cdot v_5 \cdot {v_5}^{(1)} \\ 1 & {v_1}^{(2)} & \cdots & {v_5}^{(2)} & v_1 \cdot {v_1}^{(2)} & \cdots & v_5 \cdot {v_5}^{(2)} & v_1 \cdot v_1 \cdot {v_1}^{(2)} & \cdots & v_5 \cdot v_5 \cdot {v_5}^{(2)} \\ \vdots & \vdots & \vdots & \vdots & \vdots & & & & & \\ 1 & {v_1}^{(n)} & \cdots & {v_5}^{(n)} & v_1 \cdot {v_1}^{(n)} & \cdots & v_5 \cdot {v_5}^{(n)} & v_1 \cdot v_1 \cdot {v_1}^{(n)} & \cdots & v_5 \cdot v_5 \cdot {v_5}^{(n)} \end{bmatrix} \tag{13}$$

$$\begin{aligned} \underset{\vec{g}}{\text{minimize}} \quad & \sum_{i=1}^{n} \left(\hat{d}_j - d_j \right)^2 \\ \text{subject to} \quad & \hat{d}_j \succeq 0 \end{aligned} \tag{14}$$

3. Simulation and Results

The simulation procedure consists of estimation for 2D position of a mobile node in a room of 3x3x3 m. The parameters used for the channel model, transmitters, and receiver are exposed in table 1. Other parameters as noise, PD responsivity and so on, are available in [19]. The reason to consider a FOV value different from those exposed in most cases in literature is to regard a harder situation for fitting functions with a lower FOV value. This section is divided into three-part. Each part represents one step done inside the simulation process.

Table 1
System parameters

Parameter	Value
Semi-angle Half power	70°
Lambertian Order	1
Source power	$10\,(W)$
Area of PD	$10^{-4}\,(m^2)$
$T_s(\psi_{ij})$	1
Half angle FOV receiver	60°
Room dimensions	$3 \times 3\,(m)$
LED height	$3\,(m)$
$g(\psi_{ij})$	1
Number of LEDs	4
PD height	$1\,(m)$
x-y Grid step	$0.1\,(m)$

3.1. Fitting Functions Performance

First step in simulation process consisted on finding the coefficients of polynomial functions. As we showed before, this coefficients were calculated from NLLS algorithm. For forming the matrix D a mobile node is positioned in 361 different points over the grid, due to grid step is $0.1\,m$. This value is considered at the most cases of VLP simulations on literature). For each grid point, the used tilted angles were $\beta = [-15^{\circ}, -10^{\circ}, -5^{\circ}, 0^{\circ}, 5^{\circ}, 10^{\circ}, 15^{\circ}]$. This means, we used a total of 2527 point cases and represent all possibilities of vector $\vec{v}$. For each angle case of vector $\vec{v}$, its available the true distance d_j and all the true distances conform the vector F. With Matrix D and vector $\vec{F}$, are introduced to polynomial fitting matlab function available in [20]. We took the 60% of available data in a randomly form. The training step was made with perfect tilted angles. After the training step, we validated three fitted function (linear, quadratic and cubic). With 40% of remaining data a validation step was done. In table 2 is possible to observe the performance from three fitted functions. The error corresponds to absolute difference between the estimated distance and correct distance. Third order function presents a mean and deviation error less than $0,1\,cm$. Second order polynomial present a best performance than first order, but all the proposer polynomial have error less than $5\,cm$ in distance estimation.

Table 2
Training Step: Error of distance estimation by fitting functions

Index	Error(m) $\hat{d}_1$	Error(m) $\hat{d}_2$	Error(m) $\hat{d}_3$	Error(m) $\hat{d}_4$
Mean 1st	$0,0433$	$0,0425$	$0,0434$	$0,0426$
Std 1st	$0,0308$	$0,0310$	$0,0313$	$0,0323$
Mean 2nd	$0,0105$	$0,0100$	$0,0098$	$0,0100$
Std 2nd	$0,0107$	$0,0103$	$0,0105$	$0,0103$
Mean 3th	$7,406 \cdot 10^{-4}$	$7,559 \cdot 10^{-4}$	$9,5 \cdot 10^{-4}$	$8.88 \cdot 10^{-4}$
Std 3th	$0,0021$	$0,0012$	$0,0019$	$0,0020$

Once the fitted functions are ready, the next step is test them in VLP system. To do this, the same 361 grid points are used, but now, PD noise is included. For each grid point simulation is repeated 10 times include the noise effect. The results are summarised in table 3. Again the best performance corresponds to third order polynomial with errors less than 2 *cm*.

Table 3
Positioning Errors with perfect angle

Index	Mean(m),15°	Std(m),15°	Mean(m), 10°	Std(m),10°
1st	0, 0324	0, 0337	0, 0249	0, 0258
2nd	0, 0273	0, 0326	0, 0187	0, 0196
3th	0, 0117	0, 0094	0, 094	0, 0068

In figures 4a and 4b are plotted the cumulative distribution of positioning. The behaviour in first and second order functions are similar, but third order presents less CDF. In figures 5a and 5b are plotted the positing distribution of estimated coordinates for the best case: third order function.

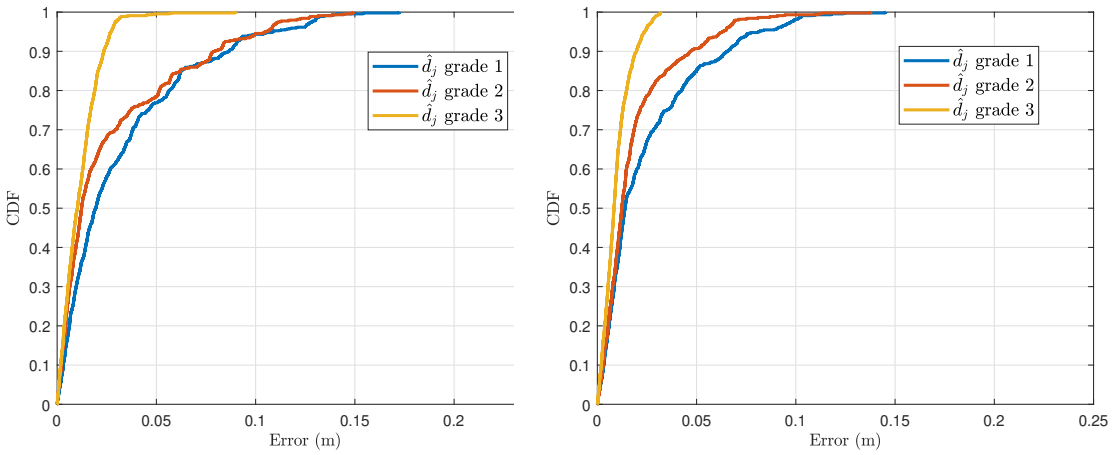

(a) $\beta = 15^{\circ}$ (b) $\beta = 10^{\circ}$

Figure 4: CDF for fit functions with exact β

3.2. Effect on mismatch tilt measurement

In contrast with previous scenario, now we consider a deviation in tilted angle to discover his influence on polynomial functions and VLP system. To characterise the behaviour of non perfect tilted angle, we used an IMU sensor model MPU9250. An Arduino Nano platform was used to recorder the IMU data, process it and calculate the orientations angles. For calculations a code library was employed available in [21]. Samples recorder consisted in hold the sensor with a hand (as a cellphone) and tilted the sensor up to get 15°. This angle was measured with a standard inclinometer OOTDTY-8YY00146. Figure 6 shows the distribution of non perfect angle

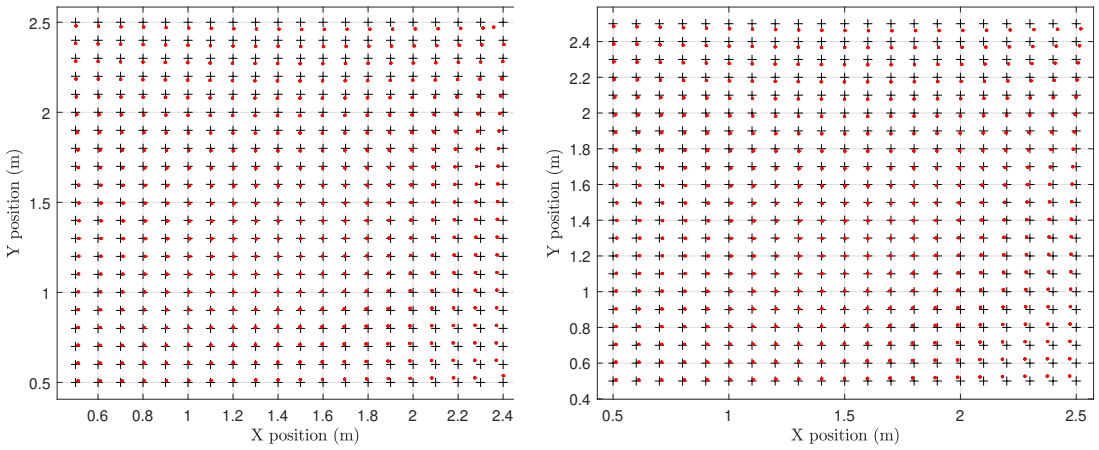

(a) $\beta = 15^{\circ}$ (b) $\beta = 10^{\circ}$

Figure 5: Estimated position with 3th order function β.
"+":Ideal Position "•":Estimated Position

around 15°. The natural hand move delivers a standard deviation of 1.5° and a mean value of 0.5°. Because the samples form a normal distribution, this model is used to provided the non perfect angle to simulation step.

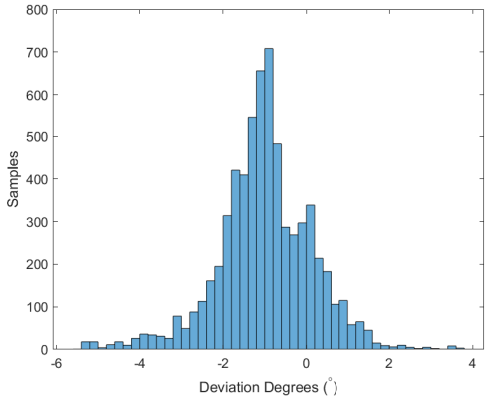

Figure 6: Tilted PD angle deviation distribution $\sigma = 1.5^{\circ}$,$\mu = 0.5^{\circ}$

In table 4 there are the error of positioning system consider a non perfect tilted angle. The third order once more has the best performance, but the difference between the other polynomials has become less with an mean error up to 2 *cm*. Figures 7a and 7b shows the CDF positioning error for non perfect tilted angle. Plots deliver a change on third order CDF when $\beta = 15^{\circ}$, instead of $\beta = 10^{\circ}$ three polynomials have a similar behaviour. The most evident change can be appreciate from figure 4a and 4b against figures 7a and 7b.With non exact β appears a displacement on red dots. If we focus on right corners in figure 8a appears a dispersion behaviour and this is due to

the loss Line-on-sight link from the transmitter positioned at the right side.

Table 4
Positioning Errors with non perfect angle

Index	Mean(m),15°	Std(m),15°	Mean(m), 10°	Std(m),10°
1st	0, 0384	0, 0374	0, 0323	0, 0301
2ns	0, 0388	0, 0381	0, 0289	0, 0273
3th	0, 0279	0, 0244	0, 0253	0, 0217

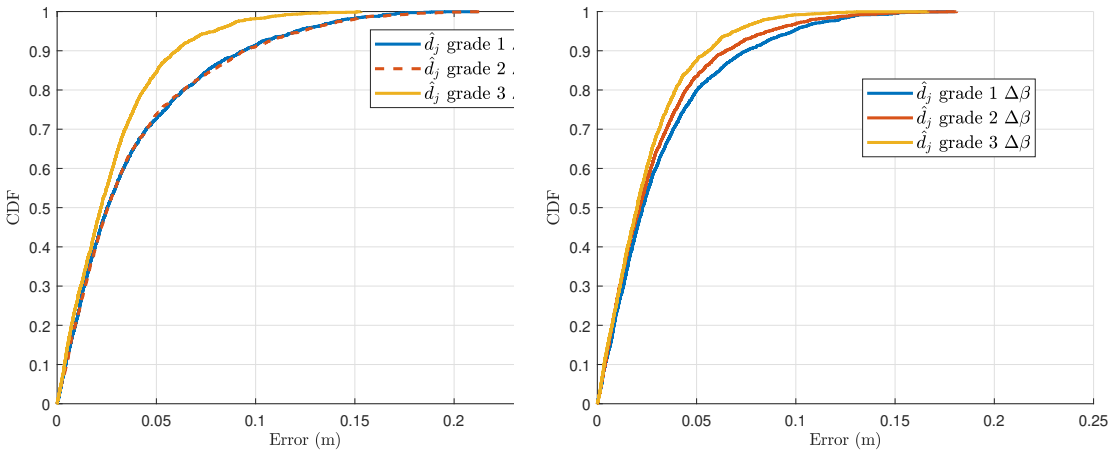

(a) $\beta = 15^{\circ}$ (b) $\beta = 10^{\circ}$

Figure 7: CDF for fit functions with non exact β

3.3. Comparing Results

With all of previous results, in table 5 shows the percent difference between perfect tilted angle and non perfect case. Negative percent means there was increment respect to the ideal case. We can infer that all polynomial are not robust to non perfect tilted angle, but the most sensible functions is third order polynomial. In fact, this function is the most accurate to estimate distance and producing less positioning error but is the less robust too β changes.

Table 5
Mean and Standard deviation error according fitting functions

Index	Mean(%),15°	Std(%),15°	Mean(%), 10°	Std(%),10°
Δ1st	−18.518	−10.979	−29.718	−16.667
Δ2nd	−42.124	−16.871	−54.545	−39.285
Δ3th	−138.461	−159.574	73.085	−219.117

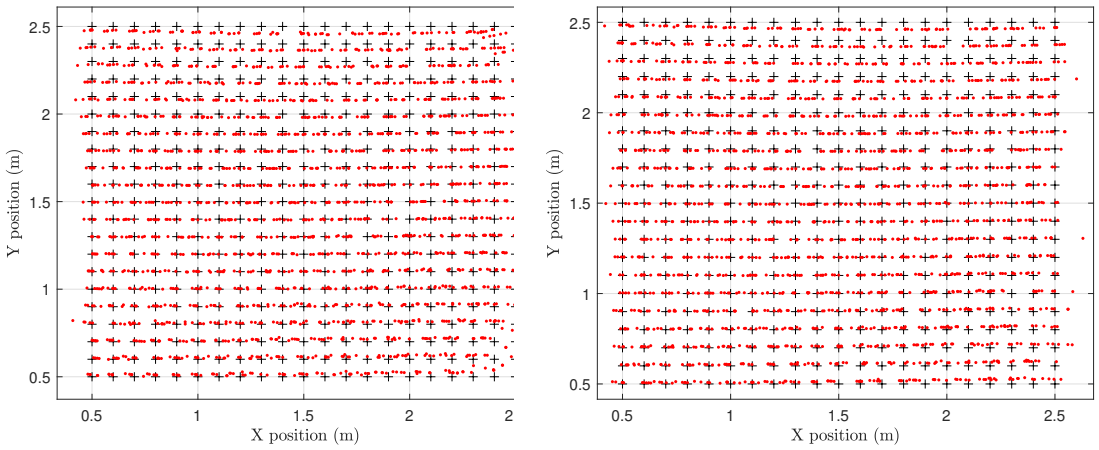

(a) $\beta = 15^{\circ}$ (b) $\beta = 10^{\circ}$

Figure 8: Estimated position with 3th order function non exact β.
"+":Ideal Position "•":Estimated Position

4. Conclusions and Future Works

In this work we proposed three polynomial fitting functions to estimate the distance from RSS in tilted PD device. The functions works under tilted angles with certain deviations. Movements could be produced by the natural move of human body, irregular plane, etc. The deviation angle has been characterised through samples recorder from real IMU sensor. The performance of these functions in VLP system has been tested by Monte-Carlo simulations. Results shows that it is possible to construct multi variable polynomial functions to approximate power versus distance with tilted receiver. Also, there are non robust behaviour from polynomial functions performance against the deviation of non perfect tilted angle, and therefore an affected performance on entire VLP system.

This approach could be tested in a real environment, using a PD located over the human's body, for example in a hospital, but with drones is possible to assure the 361 points of the grid due to great stability inside an industrial factory room. The coefficients of fitting functions will depend on the environment, existing blockages, multi-path, error in angle measurements (tilt and rotation), and Transmitter's coverage. All these factors will affect the training phase of fitting functions. In future works we pretend to extend the polynomial functions considering rotations angle (It is very important in real environments as we mentioned before) and test other kinds of fitting functions as exponential, piece-wise, and machine learning, all of this to improve the robustness against rotation changes over real experiments with embedded systems.

5. Acknowledgments

The authors acknowledge the financial support of Beca Doctorado en el Extranjero (Becas Chile) 2020 ANID (PFCHA) 72210523 and the project FONDECYT REGULAR 1211132 at the University of Santiago of Chile.

References

[1] N. Samama, Global positioning: Technologies and performance, volume 7, John Wiley & Sons, 2008.

[2] N. Chaudhary, L. N. Alves, Z. Ghassemblooy, Current trends on visible light positioning techniques, in: 2019 2nd West Asian Colloquium on Optical Wireless Communications (WACOWC), 2019, pp. 100–105. doi:10.1109/WACOWC.2019.8770211.

[3] J. Liu, Y. Chen, A. Jaakkola, T. Hakala, J. Hyyppä, L. Chen, J. Tang, R. Chen, H. Hyyppä, The uses of ambient light for ubiquitous positioning, in: 2014 IEEE/ION Position, Location and Navigation Symposium-PLANS 2014, IEEE, 2014, pp. 102–108.

[4] M. Maheepala, A. Z. Kouzani, M. A. Joordens, Light-based indoor positioning systems: A review, IEEE Sensors Journal 20 (2020) 3971–3995. doi:10.1109/JSEN.2020.2964380.

[5] S. Shawky, M. A. El-Shimy, Z. A. El-Sahn, M. R. Rizk, M. H. Aly, Improved vlc-based indoor positioning system using a regression approach with conventional rss techniques, in: 2017 13th International Wireless Communications and Mobile Computing Conference (IWCMC), IEEE, 2017, pp. 904–909.

[6] N. Chaudhary, L. N. Alves, Z. Ghassemlooy, Impact of transmitter positioning and orientation uncertainty on rss-based visible light positioning accuracy, Sensors 21 (2021) 3044.

[7] N. Stevens, H. Steendam, Influence of transmitter and receiver orientation on the channel gain for rss ranging-based vlp, in: 2018 11th International Symposium on Communication Systems, Networks Digital Signal Processing (CSNDSP), 2018, pp. 1–5. doi:10.1109/CSNDSP.2018.8471749.

[8] N. Stevens, H. Steendam, Planar positioning bias due to transmitter and receiver tilting in rss-based ranging vlp, Optik 206 (2020) 163100. doi:https://doi.org/10.1016/j.ijleo.2019.163100.

[9] H.-S. Kim, D.-R. Kim, S.-H. Yang, Y.-H. Son, S.-K. Han, An indoor visible light communication positioning system using a rf carrier allocation technique, Journal of Lightwave Technology 31 (2013) 134–144. doi:10.1109/JLT.2012.2225826.

[10] S.-H. Yang, H.-S. Kim, Y.-H. Son, S.-K. Han, Three-dimensional visible light indoor localization using aoa and rss with multiple optical receivers, J. Lightwave Technol. 32 (2014) 2480–2485.

[11] S. Li, S. Shen, H. Steendam, A positioning algorithm for vlp in the presence of orientation uncertainty, Signal Processing 160 (2019) 13–20. doi:https://doi.org/10.1016/j.sigpro.2019.02.014.

[12] B. Zhu, Z. Zhu, Y. Wang, J. Cheng, Optimal optical omnidirectional angle-of-arrival

estimator with complementary photodiodes, Journal of Lightwave Technology 37 (2019) 2932–2945. doi:10.1109/JLT.2019.2907969.

[13] A. H. A. Bakar, T. Glass, H. Y. Tee, F. Alam, M. Legg, Accurate visible light positioning using multiple-photodiode receiver and machine learning, IEEE Transactions on Instrumentation and Measurement 70 (2021) 1–12. doi:10.1109/TIM.2020.3024526.

[14] M. Kok, T. B. Schön, A fast and robust algorithm for orientation estimation using inertial sensors, IEEE Signal Processing Letters 26 (2019) 1673–1677. doi:10.1109/LSP.2019.2943995.

[15] E. M. Diaz, D. B. Ahmed, S. Kaiser, A review of indoor localization methods based on inertial sensors, Geographical and Fingerprinting Data to Create Systems for Indoor Positioning and Indoor/Outdoor Navigation (2019) 311–333.

[16] N. Stevens, D. Plets, L. De Strycker, Monte carlo algorithm for the evaluation of the distance estimation variance in rss-based visible light positioning, in: 2017 20th International Symposium on Wireless Personal Multimedia Communications (WPMC), IEEE, 2017, pp. 212–216.

[17] D. Plets, S. Bastiaens, N. Stevens, L. Martens, W. Joseph, Monte-carlo simulation of the impact of led power uncertainty on visible light positioning accuracy, in: 2018 11th International Symposium on Communication Systems, Networks & Digital Signal Processing (CSNDSP), IEEE, 2018, pp. 1–6.

[18] Z. Ghassemlooy, W. Popoola, S. Rajbhandari, Optical wireless communications: system and channel modelling with Matlab®, CRC press, 2019.

[19] M. Kavehrad, R. Aminikashani, Visible Light Communication Based Indoor Localization, CRC Press, 2019.

[20] A. Cecen, Multivariate polynomial regression, 2021. URL: https://fr.mathworks.com/matlabcentral/fileexchange/34918-multivariate-polynomial-regression, program code ver.1.4.0.0.

[21] H. Tai, Arduino library for mpu9250 nine-axis (gyro + accelerometer + compass) mems motion tracking device, 2021. URL: https://www.arduino.cc/reference/en/libraries/mpu9250/, library code ver.0.4.2.